Engineering Fiber-Nonlinearity Based Entangled Photon Sources for Quantum Key Distribution Applications

Gregory S. Kanter,[1] Shawn X. Wang,[1] Yu-Ping Huang,[2] and Prem Kumar[2]
[1]NuCrypt LLC, 1840 Oak Avenue, Suite 212-S, Evanston, IL 60201
[2]Center for Photonic Communication and Computing, EECS Department, Northwestern University, 2145 Sheridan Rd. Evanston, IL 60208
Email: kanterg@nucrypt.net, Phone: 847-733-8750

Abstract: We model fiber parametric entangled photon sources for use in quantum key distribution applications. Effects of Raman scattered photons are evaluated and are found to be manageable when appropriately detuned optical filters are employed.

OCIS codes: (060.5565) Quantum communications, (270.5568) Quantum cryptography, (060.2330) Fiber-optic communications

1. Introduction

Quantum entangled states exhibit unique properties that cannot be described classically. In addition to their purely scientific interest, entanglement is a fundamental resource for all of quantum information processing. Entangled photons are particularly useful since they can be distributed over long distances via low-loss optical fiber, which is appealing in various applications including quantum key distribution (QKD). Parametric processes have been investigated for generating entangled light, including via nonlinear crystals [1] as well as directly in optical fiber [2]. Although the performance of entangled photon sources (EPSs) based on parametric processes such as spontaneous down-conversion has been studied extensively, the effect Raman-scattered photons from a fiber-based entanglement source would have on QKD has not received much attention. Generating entanglement directly in optical fiber has some advantages including low-loss coupling to distribution fiber, ease of manufacturability, and the ability to scale to high repetition rates. However, Raman scattering poses a potential limitation to the performance of fiber-based sources. One line of research into controlling Raman scattering employs microstructure fiber to generate entangled photon pairs separated in frequency by a large amount such that they are outside the Raman bandwidth [3]. In such a case, however, both photons of the pair are no longer at a low-loss telecommunication wavelength. Another method aims to space the wavelengths of the pairs as close as possible where the Raman scattering is relatively small and, if further reduction is necessary, to cool the fiber to low temperatures thereby reducing the phonon population [2, 4]. However, cooling the fiber can be inconvenient or impractical depending on the application. We have recently developed a comprehensive model to describe fiber-based entangled photon sources. In this work, we apply the model to investigate sources capable of generating pairs of photons in the telecommunications band. We quantify the quality of the generated entangled pairs via metrics such as two-photon-interference (TPI) fringe visibility and the QKD system metric of key distribution rate. We study how the quality of the entangled photon pairs degrades as the wavelength separation between the pump and the generated signal/idler photons changes in order to characterize the behavior of a multi-channel EPS. We find that, in many cases, cooling the fiber brings only a modest benefit, except when entangled pairs in several wavelength channels are desired from a single source.

2. Model and Results

We model a fiber-based parametric EPS in a configuration similar to that in [4] with pulsed pump operation. The temporal duration of the pump pulses is set to be $0.45/B$, where B is the bandwidth of the signal and idler optical filters. This approximates the duration of a transform-limited sub-ps pulse passing through a Gaussian filter of bandwidth B prior to pumping the nonlinear fiber. We account for photon-pair generation via both spontaneous four-wave mixing and spontaneous Raman scattering. The number of Raman photons is calculated based on the model and measurements in [5], and is both temperature and wavelength dependent. The TPI visibility and quantum bit error rate (Q_{BER}) are calculated using $(C–A)/(C+A)$ and $A/(C+A)$, respectively, where C is the number of coincidence counts when the photon pairs are measured in compatible polarization basis and A is the number of accidental coincidence counts when they are measured in incompatible basis. Dark counts from the single-photon detectors are included in A via the dark-count probability per pulse (P_{dk}). Detector after-pulse counts are accounted for by increasing the detector dark-count rate by the expected after-pulse counts calculated self-consistently for a given single-photon count level and the detector after-pulse probability. After-pulsing has a more complex dynamics than is captured by this model, but the method is adequate for low after-pulse rates (after-pulsing is set to 1-2% in all simulations). The quantum key generation rate (R) per pump pulse is calculated using typical assumptions [6]:

$$R = 2q(C + A)[1 - H_2(Q_{BER}) - f(Q_{BER})H_2(Q_{BER})] \qquad (1)$$

where q is the basis reconciliation factor (set to 0.5), $f(\varepsilon)$ is the error correction efficiency (set to 1.22), and H_2 is the binary entropy function. Mismatches in the filter center frequencies and the filter shape are not included in the simulations presented in this paper. Further details of the model will be reported in the future.

Entangled photons sources can be characterized by the relationship between the observed coincidence counts and the resulting TPI fringe visibility. Any parametric EPS will experience degradation in its TPI fringe visibility as the coincidence-count level increases due to multi-pair production, although Raman scattering can exaggerate the effect. Figure 1 (Left) shows a comparison between the model and the experimental results reported in [4]. The simulation uses a filter bandwidth of 1nm and a pump-to-signal frequency separation of 500GHz. The simulation matches the experiment well at three different fiber temperatures (295K, 193K, and 77K) when the overall detection efficiency (η_{tot}) is –11dB, which takes into account all losses from pair generation through detection including loss in the polarization beam cube, multiple filter stages, and the efficiency of the single-photon detector. The chosen temperatures correspond to the nonlinear fiber being held at room temperature, cooled using a scientific freezer, and immersed in liquid nitrogen. We have noticed that the insertion loss through the nonlinear fiber increases slightly when the fiber is cooled, which may account for the reduced number of coincidence counts seen experimentally in comparison to the simulation as the temperature is lowered. The simulated P_{dk} is set to an artificially low number (10^{-8}) since the dark counts were subtracted from this data set. The back-to-back (no additional η_{tot} degradation due to loss from fiber propagation) quantum key generation rate was calculated with a reasonable $P_{\mathrm{dk}}=10^{-5}$ and improves from $1.2\mathrm{x}10^{-5}$ at 295K to $8.6\mathrm{x}10^{-5}$ at 77K. Operating at room temperature thus reduces the key rate by about the same amount as propagating one of the entangled photons through 43km of optical fiber (assuming 0.2dB/km fiber loss). When the filter bandwidth and the pump-to-signal frequency separation are both reduced by a factor of 5 (0.2nm and 100GHz, respectively), the performance improves (due to lower Raman scattering closer to the pump wavelength) and the effect of temperature on performance is somewhat reduced, as shown in Fig. 1 (Right). The back-to-back QKD rate now increases from $3.6\mathrm{x}10^{-5}$ at 295K to $1\mathrm{x}10^{-4}$ at 77K, or equivalent to 22km of fiber propagation. This illustrates the importance of designing the optical filters appropriately. Figure 1 (Right) also shows the TPI visibility performance when the fiber is cooled to 4K (liquid Helium).

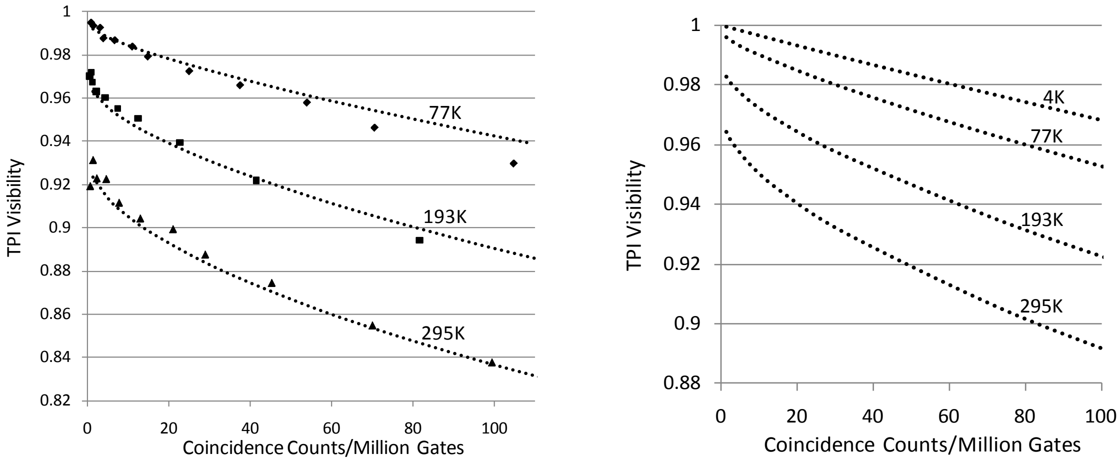

Fig. 1: (Left) TPI visibility as a function of coincidence counts (per million pulses) at three different temperatures for a 500GHz pump-to-signal separation and a 1nm filter bandwidth. The marked points are experimental data while the dotted lines are results of simulation. (Right) Similar plot showing results of simulating 100GHz separation and 0.2nm filter bandwidth.

Since the parametric nonlinearity is broad-band, a single EPS can generate photon pairs at multiple pairs of wavelengths. The ability to generate such multiple entangled photon streams could be useful for WDM quantum networks. Three such pairs have been demonstrated in a fiber based EPS with the signal wavelength adjustable over a few nm [4], while over 20nm of adjustability has been demonstrated using a second-order nonlinear medium [1]. We simulate the effect of moving the signal/idler optical filters further from the pump while keeping the center frequencies on a 100GHz frequency grid and maintaining a 0.2nm bandwidth. This simulates the performance of a wavelength-division-multiplexed (WDM) EPS. Figure 2 (Left) shows how the key-rate performance degrades as a function of the number of WDM channels. Cooling the fiber to 77K increases the number of (100GHz grid) wavelength pairs with a key generation rate $R \sim 10^{-5}$ or above from about 5 to about 15. The plot illustrates how the advantage of cooling the fiber increases in the WDM case.

Figure 2 (Right) plots the key generation rate/s (R*EPS pulse repetition rate) for a 1GHz repetition rate EPS with detectors having characteristics similar to those used in [7] having a detection efficiency of 13% ($\eta_{\text{tot}} = -12.8$dB), P_{dk} of 6.6×10^{-6}, and after-pulse probability of 2.2%. The entangled source is at room temperature with a pump-to-signal separation of 100GHz and filter bandwidth of 0.2nm. Both a symmetric (EPS placed symmetrically between the two users) and an asymmetric (all fiber loss placed on one of the entangled pairs) case is shown. The simulation suggests that even room-temperature fiber-based entangled sources, like their second-order crystal counterparts [8], can operate over fiber links of >200km when used symmetrically.

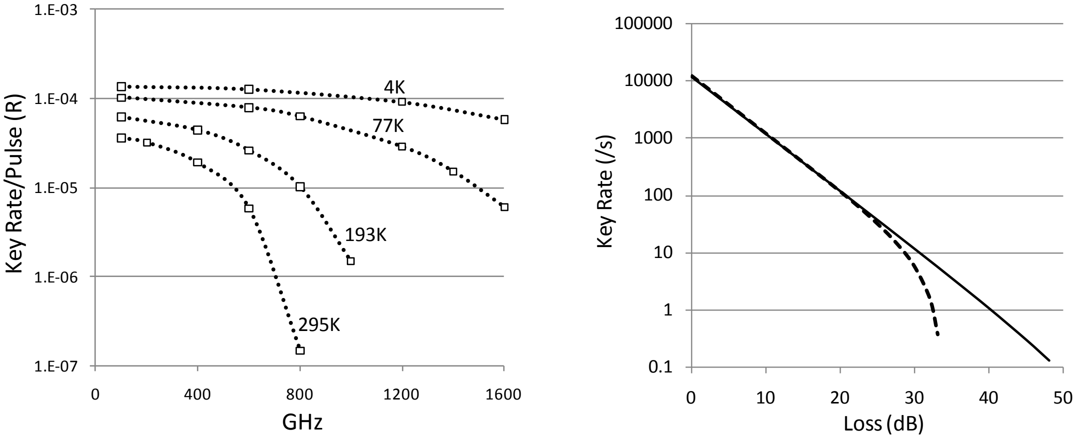

Fig. 2: (Left) Key generation rate/pulse as a function of pump-to-signal frequency separation on a 100GHz frequency grid. (Right) Key generation rate/s for a 295K-temperature EPS as a function of added insertion loss using 1GHz-rate compatible detectors. Both symmetric (solid line) and asymmetric (dashed line) configurations are plotted.

3. Summary

We have developed a comprehensive model to describe fiber-based entangled photon sources. In this paper we have used this model to evaluate entanglement-based quantum key distribution. The effect of Raman scattered photons on entanglement is quantified and different filtering schemes are evaluated. The benefit of cooling the fiber to liquid-nitrogen temperature is evaluated, and shown to be particularly important for sources which are required to emit entangled photons at multiple wavelength pairs, but markedly less important for single-channel applications. Room temperature operation of fiber-based entangled photon sources together with high-rate avalanche-photodiode based single-photon detectors can lead to QKD systems with >200km reach.

This work was supported in part by the Army Research Office and Air Force Research Laboratory, although the content does not necessarily reflect the position of the U.S. government and no endorsement should be inferred.

4. References

[1] H. C. Lim *et al.*, “Wavelength-multiplexed distribution of highly entangled photon-pairs over optical fiber,” Opt. Express **16**, 22099–22104 (2008).

[2] K. F. Lee *et al.*, “Generation of high-purity telecom-band entangled-photon pairs in dispersion-shifted fiber,” Opt. Lett. **31**, 1905–1907 (2006).

[3] J. Fan *et al.*, “Bright phase-stable broadband fiber-based source of polarization-entangled photon pairs,” Phys. Rev. A **76**, 043836 (2007).

[4] S. X. Wang and G. S. Kanter, “Robust multiwavelength all-fiber source of polarization-entangled photons with built-in analyzer alignment signal,” IEEE Sel. Topics in Quant. Electron. **15**, 1733–1740 (2009).

[5] X. Li *et al.*, “Measurement of co- and cross-polarized Raman spectra in silica fiber for small detunings,” Opt. Express **13**, 2236–2244 (2005).

[6] M. Koashi and J. Preskill, “Secure quantum key distribution with an uncharacterized source,” Phys. Rev. Lett. **90**, 057902 (2003).

[7] N. Namekata *et al.*, “Ultra-low-noise sinusoidally gated avalanche photodiode for high-speed single-photon detection at telecommunication wavelengths,” IEEE Photon. Tech. Lett. **22**, 529-531 (2010).

[8] J. F. Dynes *et al.*, “Efficient entanglement distribution over 200 kilometers,” Opt. Express **17**, 11440–11449 (2009).